Clustering of scatterers in mobile radio channels - Evaluation and modeling in the COST259 Directional Channel Model

Henrik Asplund, Andreas F. Molisch, *Senior Member, IEEE*, Martin Steinbauer, *Student Member, IEEE*, and Neelesh B. Mehta, *Member, IEEE*

***Abstract*— We analyze the clustering of scatterers in mobile radio channels, i.e, the fact that scatterers are usually not located uniformly in the whole coverage area, but tend to occur in clusters. While this has been recognized for some time, a realistic model for this phenomenon has been lacking up to now. We first analyze measurements to extract the distribution of the number of observed clusters. We then present a model that reflects not only this distribution, but also reproduces the appearance and disappearance of clusters as the mobile station moves through the cell. Our approach has been adopted as an important part of the COST259 Directional Channel Model, a standard model for directional mobile radio channels. Finally, we discuss the implications of the model for the system performance of CDMA and SDMA systems.**

***Index Terms*— channel model, clusters, direction-of-arrival**

I. Introduction

For the design and performance evaluation of mobile radio systems, realistic channel models are an absolute prerequisite. As systems become more elaborate, the requirements for channel models also change. For first- and second-generation systems, the Okomura-Hata field-strength model [1] and the wideband GSM channel model derived by the European research initiative COST 207 [2] have been sufficient. However, these models cannot be applied confidently to third- and fourth-generation systems.

A major shortcoming of the old models is the treatment of "clustering" of scatterers. In any wireless channel, scatterers are not distributed uniformly throughout the whole coverage area, but rather occur in clusters. One cluster of scatterers is always located around the mobile station [3], [4]. Other clusters (henceforth called "far clusters") correspond to high-rise buildings in urban environments, and hills/mountains in rural environments [5]. In general, far clusters lead to a significant increase in the delay and angular dispersion, and thus have a considerable influence on systems with large bandwidth and/or smart antennas.

Far clusters carry significant power mostly when they have line-of-sight (LOS) both to the base station (BS) and the mobile station (MS). As the MS moves through the cell, its LOS to the far scatterers might disappear at some point. This dynamic behavior of the clusters is especially relevant for the performance of channel trackers, again both in the delay domain (Rake receivers or equalizers) and the spatial domain (smart antennas).

Many of the older channel models (see [6], [7] for an overview) ignore the far clusters, or try to incorporate the increased dispersion by modifying the properties of the cluster around the MS. The GSM channel models actually include one far scatterer cluster,[1] but assume that the (small-scale-averaged) power and the excess delay (relative to the first cluster) are constant. The first 3GPP channel models [8] tried to remedy that situation by introducing long-term variations of the power of the second cluster. However, the excess delay is still constant, and no specifications are given for the angular properties of the clusters.

In this paper, we present a model that overcomes all these shortcomings, and allows a realistic simulation of cluster properties. The model is based on a geometrical approach, and introduces the concept of "visibility regions" and "transition functions" to accurately model the dynamic behavior of clusters. We show what parameters are needed for a complete specification of the model, and extract the parameter values for macrocells from measurements.

Our model is an important part of the COST259 Direction Channel Model (DCM), a comprehensive channel model for third- and fourth generation systems [9], [10]. It was created by a subgroup of COST 259 [11] (in which the authors of this paper played a major role), and approved by its general assembly. It has also been adopted (in simplified form) for the standardization of UMTS [12].

The paper is organized as follows. In Section II, we describe the geometrical approach for the modeling of the cluster position. Next, we explain the concept of visibility regions and transition functions that form the basis for the description of the dynamic behavior (appearance and disappearance) of the clusters. We also derive a set of parameters that specifies the inter-cluster properties, and extract the values of these parameters for the macrocellular case. These values have been adopted for the use in the COST259 DCM. Section IV discusses the influence of the clusters on system behavior, and presents some simulation results that prove the validity of our concept and parameterization. A summary concludes the paper.

H. Asplund is with Ericsson Radio Research, Stockholm, Sweden. A. F. Molisch is with the "Wireless Systems Research Department", AT&T Labs - Research, 200 Laurel Av., Middeltown, NJ, USA. E-mail: afm@research.att.com. Martin Steinbauer was with INTHF, TU Wien. Neelesh B. Mehta is with AT&T Labs - Research, Middletown, NJ.

[1] in two of the four specified environments

0-7803-7400-2/02/$17.00 © 2002 IEEE

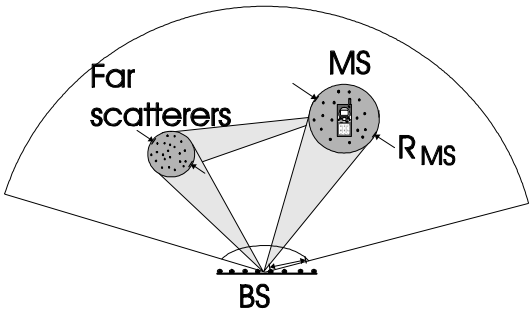

Fig. 1. Near and far scatterer clusters.

II. Geometrical approach and cluster location

A. Definition of clusters

In general, the directionally resolved impulse response can be written as

$$\underline{h}(\vec{r},\tau,\Omega,\Psi) = \sum_{\ell=1}^{L(\vec{r})} \underline{h}_\ell(\vec{r},\tau,\Omega,\Psi). \quad (1)$$

where $\vec{r}$ is the position of the receiver, τ the delay, and Ω and Ψ the directions of the multipath components at transmitter and receiver, respectively. $\underline{h}_\ell$ signifies the contribution of the ℓ-th (out of L) multipath component to the total (vector) impulse response $\underline{h}$.

It has been often observed that the scatterers are not distributed uniformly throughout the coverage area, but that they occur in clusters, see Fig. 1. In that case, it is advantageous to write Eq. (1) as

$$\underline{h}(\vec{r},\tau,\Omega,\Psi) = \sum_{m=1}^{M} \sum_{n\,\in\, C_m} \underline{h}_n(\vec{r},\tau,\Omega,\Psi). \quad (2)$$

where the multipath components $\underline{h}_\ell(\vec{r},\tau,\Omega,\Psi)$, $\ell = 1,\ldots,L$ have been grouped into $M \leq L$ *disjoint* classes (or clusters)

A cluster can thus be defined as a group of waves with similar τ, Ω,Ψ. However, we stress that it is not possible to give a mathematically unique definition of a cluster from one measurement, or even from a series of measurements in a small area. Defining an arbitrary threshold, or using human intuition, is required to uniquely define the cluster boundary. In the following, we will distinguish between inter-cluster properties, (i.e., the relative delays and angular dispersion *between* the clusters), and intra-cluster properties (i.e., the delay and angular dispersion *within* a cluster).

B. Number of clusters

The most important parameter for modeling clusters is the average number of clusters occurring in the impulse response. This value depends on the geographical and morphological properties of the propagation environment. Flat terrains with regular building structures lead to fewer clusters than, for example, a city with a few downtown skyscrapers. We thus distinguish between different "radio environments". In the COST259 channel model, the macrocellular environments are called "Generalized Typical Urban" (GTU), "Generalized Bad Urban (GBU), Generalized Rural Area (GRA), and "Generalized Hilly Terrain" (GHT).[2]

In order to obtain the average number of clusters in the different environments, measurement campaigns were performed and evaluated. One such campaign used the TSUNAMI II testbed [13] to measure impulse responses[3] in the cities of Aarhus, Denmark and Stockholm, Sweden, and in the Danish countryside. Another study used directionally resolved measurements in the city of Helsinki [14] using a channel sounder developed by the IRC of Helsinki University of Technology. Another source from the literature was the directionally resolved measurements by Martin [15] in Frankfurt, using a modified RUSK channel sounder. In all cases, the number of clusters was obtained by visual inspection. As an example, Table 1 shows the values obtained in the Danish/Swedish measurement campaign. We note that Stockholm and Frankfurt show an especially irregular building structure. In Stockholm, the irregularities are caused by large areas of water separating the built-up areas; in Frankfurt, by the combination of a few skyscrapers (higher than 100m) with "normal" European downtown and suburban buildings (height around 20-30m). Aarhus and Helsinki, on the other hand, exhibit a "typical urban" structure with a regular morphology. The Danish countryside is a "rural area" without any hills. The more frequent occurrence of far clusters in "hilly terrain" (which comprises both hilly and mountainous regions) was concluded from [16] and [17]. An average number of clusters of $N_c = 2$ was concluded from those measurements. However, we note that in these cases, only a few exemplary measurements were available. The statistical reliability of the mean number of clusters in this environment is thus comparatively low.

Environment	Fraction	of meas.	time with	Av. numb.
	1 clust.	2 clust.	3 clust.	of clust. N_c
Bad Urban	0.27	0.28	0.45	2.18
Typ. Urban	0.87	0.09	0.04	1.17
Suburban	0.92	0.08	0.00	1.08
Rural	0.94	0.06	0.00	1.06

Table I Experimentally observed number of clusters

Thus, the average number of clusters N_c in the four radio environments are

$$N_c = \begin{cases} 1.17 & GTU \\ 2.18 & GBU \\ 1.06 & GRA \\ 2 & GHT \end{cases} \quad (3)$$

[2]these names were chosen to show that the morphology of these environments is defined similar as that of the radio environments in the GSM models. The word "generalized" was included in order to indicate that many propagation effects are modeled that were neglected in the GSM models.

[3]The evaluation of this campaign did not consider directional information.

C. Location of far clusters

The next step is to model statistically the location of the far clusters (the local cluster is always around the MS). The area over which the far scatterers are distributed can be quite a bit larger than a cell area. While typical rural cell sizes have a $3-8$ km cell radius, excess delays of up to $80\mu s$ (corresponding to 12 km far scatterer distance) have been observed [18], [17]. However, the farther away the far cluster is from the BS, the less likely it becomes that it has a LOS to the BS. Secondly, BS antennas are usually placed in such a way that there are no large scatterers in the immediate surroundings. We thus model the probability density function of the distance between BS and far scatterers as an exponential distribution for the radial distance r_c of the cluster from the base station (and uniform in azimuth)

$$f(r_c, \varphi_c) = \begin{cases} 0 & r_c < r_{\min} \\ \frac{1}{2\pi\sigma_r} \exp(-\frac{r_c - r_{\min}}{\sigma_r}) & r_c \geq r_{\min} \end{cases} \quad (4)$$

The parameters $r_{\min}$, σ_r are given in Table 2 (the parameter $\sigma_{\varphi C}$ will be explained below).

	GTU/GBU	GRA/GHT
$\mathrm{r}_{\min}$ $[m]$	1000	1000
σ_r $[m]$	1500	5000
$\sigma_{\varphi C}$ [deg]	60	60

Table II Cluster position parameters

D. Cluster power

We expect the cluster power P_m to be conditioned on the excess delay $\tau_m - \tau_1$, where τ_1 is the delay of the first arriving cluster, since the extra path length and scattering gives rise to an added attenuation. Saleh and Valenzuela [19] found that a model where cluster powers decay exponentially with excess delay gave a good fit to indoor measurement data. We modify this model by not considering clusters with very weak power. The cluster power decays exponentially only up to excess delay τ_B, beyond which it remains constant. Rather, the probability that a cluster with a large delay occurs goes down (see Sec. II.C). This agrees better with the observation that sometimes, high powers of far-away clusters *do* occur, but that these occurences are rare. The cluster power model can thus be formulated as

$$P_m = A_m^2 P_{NLOS} 10^{-\frac{k_c \min(\tau_m - \tau_1, \tau_B)}{10}}, \quad (5)$$

where P_{NLOS} is the non-LOS path gain, and A_m is the transition function for activating/deactivating a cluster described in Sec III.C. The parameters k_c and τ_B characterize the power conditioned on the excess delay $\tau_m - \tau_1$ as shown in Fig. 2. In addition to this delay-dependent shadowing, every cluster (including the first one) undergoes shadowing. As a first approximation, the shadowing can be considered independent for the different clusters. The shadowing is assumed to be lognormal with a variance of 6dB.

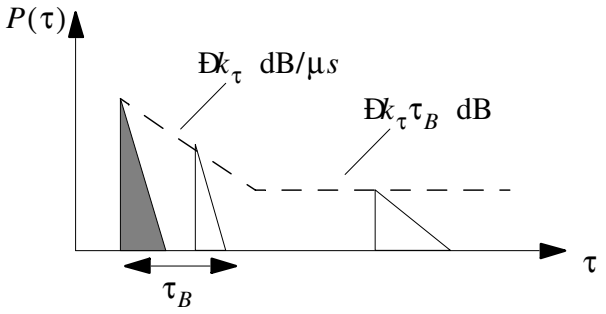

Fig. 2. Cluster power conditioned on excess delay

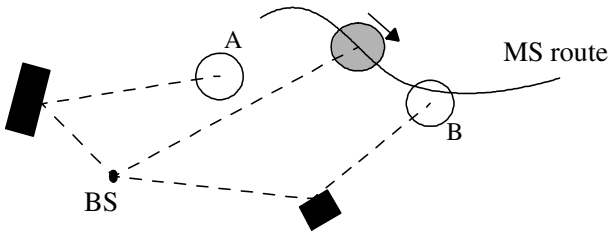

Fig. 3. Example of visibility regions (white circles) and cluster positions (black rectangles). The shaded circle is the local scattering cluster which moves with the mobile station (MS). Along the particular MS route shown, only one of the two clusters (the one associated with visibility region B) will be activated.

III. Cluster appearance and disappearance

A. The concept of visibility regions

In order to determine which far clusters can actually be seen by a mobile at a certain location, we introduce the concept of visibility regions. A visibility region is a (circular) area of radius R_c. The idea is that each time a mobile enters a visibility region, the corresponding cluster is made active, and when the mobile leaves the region the cluster will be deactivated again (see Fig.3).[4] The density of visibility regions has to be chosen in such a way that the expected value of active clusters agrees with the average number N_c specified in Sec. II.B.

We also note that due to the random placing of the far clusters and the visibility regions, the number of "currently active" clusters is a random variable. To a first approximation, it follows a Poisson distribution.

B. Placement of visibility regions

The placement of the visibility regions is one of the most intricate parts of the model. It has to be done in such a way that the following observations are fulfilled:

1) Each far cluster can be associated with several visibility regions. For example, a high-rise building can be seen from different locations in the street. The number of visibility regions associated with each cluster is modeled as a Poisson-distributed variable with mean value of two.[5]

[4] This definition would actually lead to a "hard onset" of far clusters; we will show in Sec. III.C how the transition can be made smooth

[5] The probability that two visibility regions associated with one certain far cluster overlap is so small that it does not significantly influence the mean number of visibility regions seen.

2) Visibility is more probable if the BS, MS, and far cluster are all aligned along a straight line, and becomes less likely in a broadside scenario. For example, the walls of a street canyon would block the view of a far cluster even if the BS is clearly visible along the street canyon along which the MS is located. We found that a Gaussian distribution for the angular pdf, with a spread of 60 degrees, gives good agreement with experimental values. We also found that the pdf of the density of visibility regions is approximately independent of the radial distance from the BS.
3) The density of visibility regions must be chosen in such a way that the average number of active clusters is equal to N_c.

The above requirements are fulfilled by taking the number of far cluster as

$$\frac{N_c - 1}{2} \frac{R_{cell}^2}{(R_c - L_c)^2} \tag{6}$$

with a distribution following Eq. 4, where R_{cell} is the cell radius. For each cluster, we have N_{vbpc} visibility regions, where N_{vbpc} is Poisson distributed with mean value 2, and the pdf of the visibility region location within the cell is

$$f_C(r, \phi) = \frac{2r}{R_{cell}^2} \frac{\exp\left[-\frac{(\phi - \phi_C)^2}{2\sigma_{\varphi,C}^2}\right]}{\sqrt{2\pi}\sigma_{\varphi,C}} \tag{7}$$

where $\sigma_{\varphi,C}$ is given in Table 2, and ϕ_C is the angle of the cluster as seen from the BS.

C. Transition functions

As mentioned above, defining the visibility region as circular regions that activate a far cluster as soon as the MS enters it leads to a hard activation of clusters. A smooth transition from non-active to active cluster is achieved by scaling the power of the cluster by a factor A_m^2. The transition function used is given as

$$A_m(r_{MS}) = \frac{1}{2} - \frac{1}{\pi} \arctan\left(\frac{2\sqrt{2}y}{\sqrt{\lambda x}}\right) \tag{8}$$

with

$$y = L_c - |\overrightarrow{r}_{MS} - \overrightarrow{r}_m| - R_c \tag{9}$$

$$x = L_c \tag{10}$$

where $\overrightarrow{r}_m$ is the center of the circular visibility area and λ is the wavelength. If the argument of the $arctan$ becomes larger than 300, A is set equal to zero. This function was selected as an approximation to the Fresnel function. The parameter L_c can be interpreted as the width of the transition region (see Fig. 4). Reasonable values for R_c and L_c might be on the order of the size of a city block and the width of a street respectively. In rural areas the variation in clustering is expected to be slower due to the lack of buildings. Suggested values for the macrocell radio environments are given in Table 3.

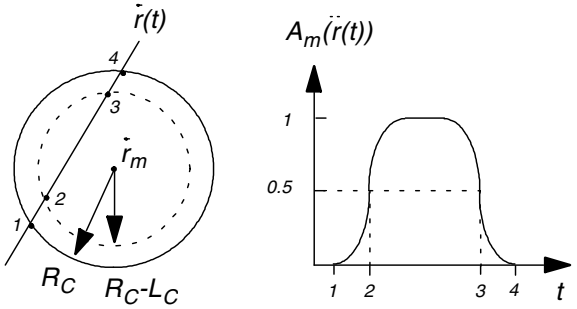

Fig. 4. Activation of cluster using a visibility area and the transition function

	GTU/GBU	GRA/GHT
R_c [m]	100	300
L_C [m]	20	20

Table III Suggested values for the clustering model.

IV. Results

A. The COST259 DCM

As mentioned in the introduction, our cluster model is an important part of the COST259 directional channel model (DCM). Our choices for cluster position and power, as well as the visibility regions and transition functions, have become part of this widely-used standard. Of course, the parameters described here do not constitute the complete model, which is much more extensive. Due to space constraints, we could not treat the intra-cluster spreads, line-of-sight components, polarization, etc. For a complete description of these aspects, the interested reader is referred to [9], [10]. Furthermore, micro- and picocells use a somewhat different clustering model [20].

B. Influence on system design

The far clusters have an important influence on systems with smart antennas, as well as on wideband systems. For wideband systems, it is a widespread misconception that the delay spread is the decisive parameter. For this reason, power delay profiles with a single-exponential decay are commonly used for channel modeling; the decay time constant is adjusted to give the same delay spread as measurement results. We enumerate below just a few examples of systems that show a big difference for the two channel models:

- *Equalizers with unequal tap spacing*. The relative benefits of such an equalizer (for a fixed total number of taps) is much larger in the clustered model. Furthermore, the dynamics of the cluster appearance/disappearance determine the requirements for the tap-position-tracker [21].
- *Selective Rake receivers and Partial Rake receivers* [22]. These receivers select L out of N available paths. While the S-Rake selects the strongest paths, the P-Rake selects just the first arriving paths. The P-Rake is thus simpler, but gives worse results. The performance degradation of the P-Rake is much larger in clustered than in single-exponential channels.

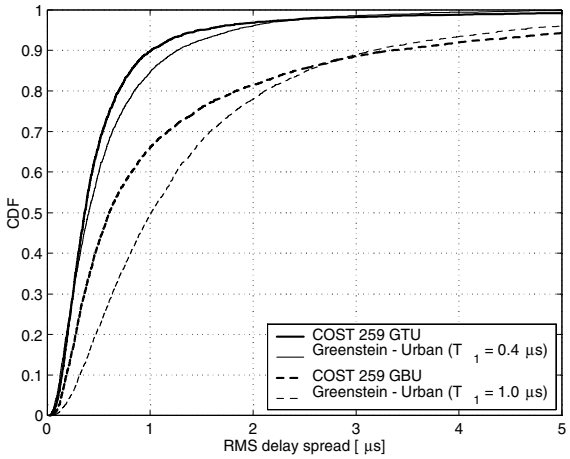

Fig. 5. Comparison of simulated rms delay spread distributions at a distance of $1km$ with the model by Greenstein. The curves for the Greenstein model have been calculated using T_1 of 0.4 μs and 1.0 μs respectively, and with $\sigma_y = 4dB$.

- *Downlink beamforming.* Knowledge of the directions and average powers of the multipath components is used for the downlink of FDD systems with smart antennas [23]. Signals propagating via different clusters can be used for "beam diversity". Furthermore, tracking the cluster directions over many bursts is vital for reliable determination of DOAs. Thus, a simulation of such a system can be performed only with a realistic clustered channel model that also includes the directions and dynamics in a correct way.

C. Simulation of delay dispersion

To show the validity of our model, we simulated the distribution of the rms delay spread as the MS moves through a Bad Urban cell. The reason for selecting this parameter as a benchmark is the fact that it has been studied extensively in the literature, and a very detailed and accurate model by Greenstein et al. is available [24]. Figure 5 shows the delay spread distribution as computed from our model, and as computed from the Greenstein model. We see that the agreement is very good. While this of course is no proof for the validity of all aspects of our model, it is a strong indication that the essential properties of the channel have been represented correctly.

V. Summary and conclusion

We have presented a model for the clustering of scatterers in mobile radio channels. We showed that far scatterer clusters are essential for the correct modeling of many advanced wireless communications systems. Our model is based on a geometrical interpretation, and allows a realistic treatment of both cluster positions and dynamics. This is done by means of visibility regions. We extracted from measurements the parameters that specify the model. Simulations of the statistics of the delay dispersion indicate the soundness of our choices. Our model, which is part of the COST259 DCM, thus allows a realistic simulation of third- and fourth generation wireless systems.

Acknowledgements: We thank the other members of the COST259 subgroup 2.1, as well as the chairman of COST259, Prof. Luis Correia, and the chairman of workinggroup 2, Prof. Ernst Bonek. The financial support of the European Union for the COST action is gratefully acknowledged.

References

[1] M. Hata, "Empirical Formula for Propagation Loss in Land Mobile Radio Services," *IEEE Trans. on VT*, vol. 29, pp. 317–325, Aug. 1980.
[2] C. of the European Communities, *Digital land mobile radio communications - COST 207*. ECSC-EEC-EAEC, 1989.
[3] W. C. Jakes, *Microwave Mobile Communications*. IEEE Press, 1974.
[4] W. C. Y. Lee, "Effects on correlation between two mobile radio base-station antennas," *IEEE Trans. Comm.*, vol. 21, pp. 1214–1224, 1973.
[5] J. Fuhl, A. Molisch, and E. Bonek, "Unified channel model for mobile radio systems with smart antennas," *IEE Proc. Radar, Sonar and Navigation*, vol. vol. 145, no. 1, pp. 32–41, 1998.
[6] W. C. Y. Lee, *Mobile Communications Engineering*. McGraw Hill, 1982.
[7] J. D. Parsons, *The mobile radio propagation channel*. Halstead Press, 1992.
[8] European Telecommunications Standards Institute, *UMTS Radio Air Interface: FDD Mode*, 1999.
[9] A. F. Molisch, H. Asplund, R. Heddergott, M. Steinbauer, and T. Zwick, "The COST259 directional channel model - i. philosophy and general aspects," *IEEE J. Selected Areas Comm.*, p. submitted, 2001.
[10] H. Asplund, A. A. Glazunov, A. F. Molisch, K. I. Pedersen, and M. Steinbauer, "The COST259 directional channel model II - macrocells," *IEEE J. Selected Areas Comm.*, p. submitted, 2001.
[11] L. Correia (Ed.), *Wireless Flexible Personalized Communications*. Wiley, 2001.
[12] TSG RAN WG4, "Deployment aspects," Tech. Rep. 3G TR 25.493 V2.0.0, 3rd Generation Partnership Project (3GPP), 2000.
[13] P. E. Mogensen, K. I. Pedersen, F. Frederiksen, and B. Fleury, "Measurements, channel statistics, and performance of adaptive base station antennas," in *COST259/260 Joint Workshop on Spatial Channel Models and Adaptive Antennas*, pp. 63–72, 1999.
[14] M. Toeltsch, J. Laurila, A. F. Molisch, K. Kalliola, P. Vainikainen, and E. Bonek, "Spatial characterization of urban mobile radio channels," in *Proc. VTC2001 Spring*, (Rhodes, Greece), IEEE, 2001.
[15] U. Martin, "Spatio-temporal radio channel characteristics in urban macrocells," *IEE Proc. Radar, Sonar and Navigation*, vol. vol. 145, no. 1, pp. 42–49, 1998.
[16] METAMORP Consortium, "Deliverables of the METAMORP project to the european union," tech. rep., European Union, 2000.
[17] P. F. Driessen, "Multipath delay characteristics in mountainous terrain at 900 MHz," in *Proc. 42nd IEEE Vehicular Techn. Conf.*, pp. 520–523, 1992.
[18] W. Mohr, "Wideband propagation measurements of mobile radio channels in mouneainous areas in the 1800mhz frequency band," in *Proc. of IEEE 43th VTC, Secaucus, New Jersey, 1993*, vol. 1, (Priscataway New Jersey), pp. 49–52, IEEE, 1993.
[19] A. A. M. Saleh and R. R. Valenzuela, "A statistical model for indoor multipath propagation," *IEEE J. Selected Areas Comm.*, vol. 5, pp. 128–137, 1987.
[20] A. F. Molisch, J. E. Dietert, R. Heddergott, M. Steinbauer, and T. Zwick, "The COST259 directional channel model III - micro- and picocells," *J. Selected Areas Comm.*, p. to be submitted, 2001.
[21] S. Ariyavisitakul, N. R. Sollenberger, and L. J. Greenstein, "Tap-selectable decision feedback equalization," *IEEE Trans. Comm.*, vol. 45, pp. 1497–1500, 1997.
[22] M. Z. Win and G. Chrisikos, *Impact of Spreading Bandwidth and Selection Diversity Order on Rake Reception*, ch. 29. Prentice-Hall, 2001.
[23] A. Kuchar, M. Taferner, M. Tangemann, and C. Hoek, "Field trial with a GSM/DCS1800 smart antenna," in *Proc. VTC'99 Fall*, (Amsterdam, The Netherlands), pp. 42–46, Sept. 1999.
[24] L. Greenstein *et al.*, "A new path-gain/delay-spread propagation model for digital cellular channels.," *IEEE Trans. on Vehicular Techn.*, vol. 46, May 1997.